

Experimental Observation of Electronic Coupling in GaAs Lateral Quantum Dot Molecules

L. Wang,* A. Rastelli, S. Kiravittaya, M. Benyoucef, and O. G. Schmidt

*Max-Planck-Institut für Festkörperforschung,
Heisenbergstr. 1, D-70569 Stuttgart, Germany*

(Dated:)

Abstract

We report the fabrication and photoluminescence properties of laterally-coupled GaAs/AlGaAs quantum dots. The coupling in the quantum dot molecules is tuned by an external electric field. An intricate behavior, consisting of spectral line crossings and avoided crossings is observed for different molecules. Anticrossing patterns in the photoluminescence spectra provide direct evidence of the lateral coupling between two nearby quantum dots. A simple calculation suggests that the coupling is mediated by electron tunneling, through which the states of direct and indirect exciton are brought into resonance.

Coupled semiconductor quantum dots (QDs) are attracting growing interest due to their potential application as solid-state quantum gates [1, 2]. Substantial progress towards the experimental implementation of such quantum dot molecules (QDMs) has been achieved in the last few years both for electrically defined QDs (see Ref. [3] and Refs. therein) and for self-assembled, vertically-stacked QDs [4, 5, 6, 7]. In the latter case, the coupling between two structurally different QDs is controlled by applying a vertical electric field. A signature of coupling and entanglement [8] is represented by anticrossing patterns in two-dimensional maps obtained from photoluminescence (PL) spectra for different values of the external field. To explore the possibility of coupling a larger number of self-assembled QDs, investigations on lateral coupling are needed [9]. The fabrication of laterally-close QDs with well-defined properties requires special growth protocols [10, 11, 12, 13, 14, 15, 16, 17] and, while indications of lateral coupling have been reported [17, 18], anticrossing patterns for lateral QDMs have not been observed so far.

In this Letter we employ a lateral electric field to tune the coupling between two laterally-close GaAs/AlGaAs QDs and present the observation of an anticrossing pattern in the PL spectra of a single GaAs QDM.

The QDM samples are grown by molecular beam epitaxy (MBE) combined with a method based on AsBr₃ selective etching of buried InAs QDs and subsequent overgrowth. With a proper choice of etching and overgrowth parameters, either single AlGaAs holes [19] or biholes aligned in the [110] direction can be created, which are used as templates for the fabrication of either single QDs or QDMs. To create QDMs, low density ($\lesssim 10^8$ cm⁻²) InAs QDs are first deposited at a substrate temperature of 500°C on a GaAs buffer, followed by a 30 s growth interruption. The substrate temperature is lowered to 470°C and 10 nm GaAs are deposited while ramping the temperature back to 500°C. An *in situ* etching step with a nominal depth of 7.5 nm is then applied to remove the buried QDs and obtain bow-tie shaped nanoholes [11, 20], which are overgrown with 10 nm Al_{0.45}Ga_{0.55}As. During Al_{0.45}Ga_{0.55}As growth, single holes are found to split into two closely-spaced holes aligned in the [110] direction. The biholes are subsequently filled by depositing 1 nm GaAs followed by a 1 min growth interruption. 100 nm Al_{0.35}Ga_{0.65}As, 20 nm Al_{0.45}Ga_{0.55}As, and 10 nm GaAs complete the structure. The GaAs-filled biholes embedded in AlGaAs represent QDMs below a thin quantum well. Atomic force microscopy (AFM) in tapping mode is employed for the morphological investigation of the bihole structure. For this purpose, the sample is

cooled to room temperature immediately after the growth of the 10 nm $\text{Al}_{0.45}\text{Ga}_{0.55}\text{As}$ layer. Because of fluctuations inherent in the self-assembled growth, the two QDs are generally not identical and their mutual coupling can be controlled by an electric field parallel to the $[110]$ direction. To this end, interdigital gate electrodes with 100/20 nm thick Au/Ti stripes and 30 μm spacing are processed on the sample surface. Micro-PL ($\mu\text{-PL}$) spectroscopy of single QDMs is performed by using a laser excitation energy of 2.33 eV. The PL is analyzed by a 750 mm focal-length spectrometer equipped with a Si charge-coupled device.

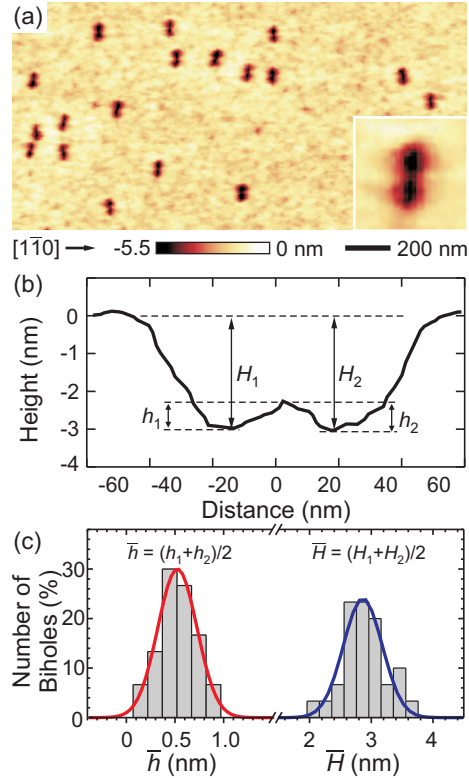


FIG. 1: (a) AFM image of biholes on the AlGaAs surface. The inset is a $125 \times 125 \text{ nm}^2$ zoom of a bihole. (b) Linescan of a bihole along the $[110]$ direction. (c) Statistical analysis of hole depth and barrier height for biholes.

Figure 1(a) shows an AFM image of biholes on the surface of the 10 nm $\text{Al}_{0.45}\text{Ga}_{0.55}\text{As}$ layer. The two holes are normally slightly different in size and shape, but are invariably aligned in the $[110]$ direction. A typical linescan of a bihole along the $[110]$ direction is displayed in Fig. 1(b). The two holes have an average center-to-center distance of 35 ± 4 nm and are separated by a thin barrier [see also the inset in Fig. 1(a)]. Figure 1(c) shows a statistical analysis of the hole depth and barrier height for the biholes. Gaussian fits to the

histograms show that the average depth and barrier height of the biholes are 2.9 nm and 0.52 nm, respectively. When the biholes are filled with GaAs and annealed for 1 min, the deposited GaAs diffuses into the biholes, thus forming inverted lateral GaAs QDMs aligned in the $[110]$ direction.

Typical PL spectra of three independent QDMs at relatively low excitation power are shown in Fig. 2(a). Different QDMs exhibit several common spectral features, which indicate that the created QDMs have similar properties. The high-energy peaks, labeled as X^0 , are attributed to the recombination of an electron and a hole confined in the larger QD composing a QDM (direct neutral exciton). Another intense peaks X^* , well separated (>3 meV) from the X^0 line, is present in all spectra. Since the background doping in our samples is p-type, we tentatively assign X^* to a positive trion. Other features, generally labelled as multi-excitons (mX) are also observed.

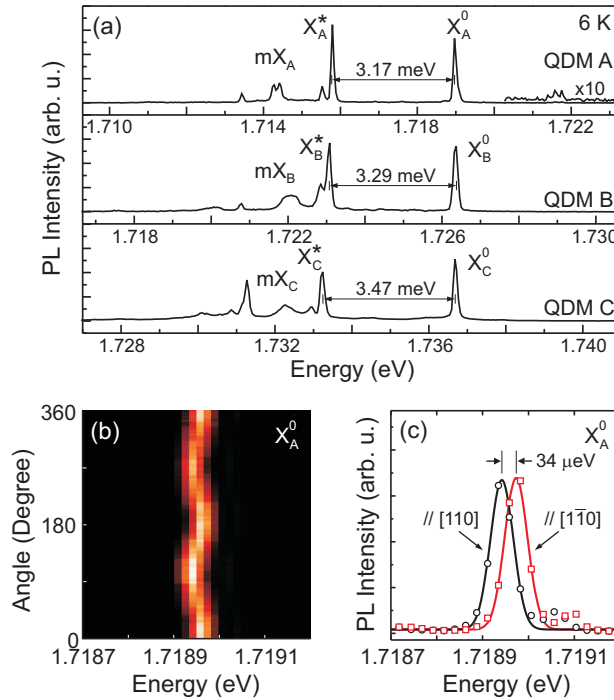


FIG. 2: (a) μ -PL spectra of three different QDMs. The energy axes are shifted to facilitate the comparison. (b) Polarization dependent PL of the neutral exciton line in QDM A. (c) PL spectra at the polarization angle of 0° and 90° . The shift of the peak position is due to the fine structure splitting of the neutral exciton line for QDM A. Note that the spectra are fitted with Lorentzian functions.

We now concentrate on the QDM A [topmost spectrum in Fig. 2(a)]. To confirm our

identification of the spectral lines, a polarization-dependent PL measurement is performed by inserting a rotatable lambda-half waveplate and a fixed Glan-Thompson polarizer in front of the spectrometer. The oscillating peak energy as a function of polarization angle in Fig. 2(b) indicates that the line X^0 originates from a neutral exciton transition [21]. The two components of the line X_A^0 , corresponding to light polarized in the $[110]$ and $[1\bar{1}0]$ directions, are plotted in Fig. 2(c). The fine structure splitting deduced from the spectra is $34 \mu\text{eV}$, which is comparable to the values typically observed for “natural” GaAs QDs [22]. Moreover, all other main lines do not show any polarization dependence, which suggests that they originate from charged excitons of direct or indirect nature [21].

Due to the slightly different size and shape of the two QDs in a QDM, we expect that the X_A^0 emission originates from the recombination of excitons in the larger dot. The recombination of electron (hole) in the large dot with hole (electron) in the small dot is suppressed, leading to a very weak signal in the PL spectra [see the weak features at 1.721-1.722 eV in the QDM A spectrum in Fig. 2(a)]. However, when the QDM is subject to an electric field, the emission of the QDM can be tuned through the quantum confined Stark effect (QCSE), and therefore the interdot coupling can also be tuned. The geometry of the Schottky interdigital electrodes processed on the sample surface is shown in Fig. 3(a). A voltage $\pm V_a$ applied to nearby electrodes produces the desired electric field along the $[110]$ crystal direction.

In order to locate QDM A with respect to the electrodes, we record PL spectra while scanning the laser spot on the sample surface. (In the experiment the sample is moved in a raster scan while the excitation/collection optics remain fixed.) The signal is then integrated over the spectral range of the QDM emission and a corresponding PL intensity-map is displayed in Fig. 3(b). From this map, we clearly see that the bright spot in the center of the image, associated with the emission of QDM A, is located about $2 \mu\text{m}$ away from one of the Ti/Au electrodes. Another spot (on the right hand side of QDM A) from another QDM is also visible.

While the contact structure employed here is easy to implement and has previously been used to apply a lateral field on QD structures [17, 23, 24], the relation between applied voltage V_a and electric field is not trivial. To clarify this point, the sample structure is simplified as a two-dimensional geometry shown in Fig. 3(c). The GaAs material parameters with a p-type doping of 10^{15} cm^{-3} (typical background doping level in our MBE chamber)

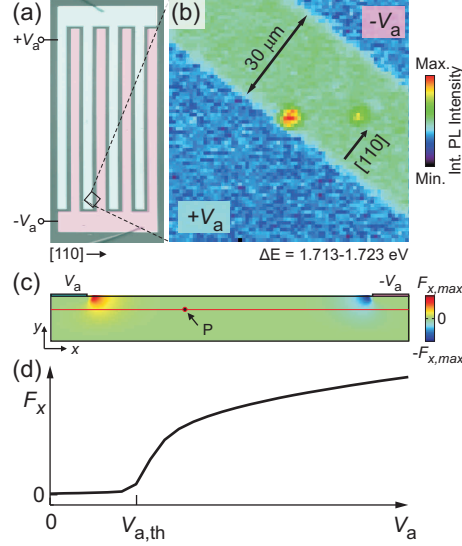


FIG. 3: (a) Optical microscopy image of the interdigital Ti/Au gate electrodes on the sample surface. The height to width ratio of the image is 2.5. (b) Integrated PL intensity map indicating the position of QDM A close to an electrode. (c) Geometry of the simplified structure used to estimate the lateral electric field F_X as a function of applied voltage V_a . (d) Relation between F_X and V_a at the point P in (c).

are assumed throughout the structure and the Schottky contacts are modeled as heavily n-type doping regions (10^{19} cm^{-3}). The Poisson equation and the carriers' (electron and hole) diffusion equations are simultaneously solved [25]. At $V_a=0$, the built-in field along the x -direction F_X in the depletion regions can be clearly seen, as color-encoded in Fig. 3(c). When the voltage is applied, the depletion region around the left electrode extends laterally and the maximum field strength increases. Figure 3(d) shows the behavior of F_X at a point P near the positively biased electrode ($1.5\ \mu\text{m}$ from the electrode and 150 nm below the surface). The result suggests that F_X increases slowly until, at a certain threshold value of the voltage ($V_{a,th}$), the depletion region reaches P. At that point the field increases abruptly. Therefore we expect that a pronounced QCSE will be observed only when $V_a > V_{a,th}$, with $V_{a,th}$ depending on the distance between QDM and the contact. This finding is in qualitative agreement with the experimental observation that only QDMs close to one of the contacts display a variation of the emission for V_a less than about 100 V .

The first effect produced by moderate fields is a slight blue-shift (of the order of $100\ \mu\text{eV}$) of most of the QDM lines. This behavior, which we observed for all the investigated QDMs

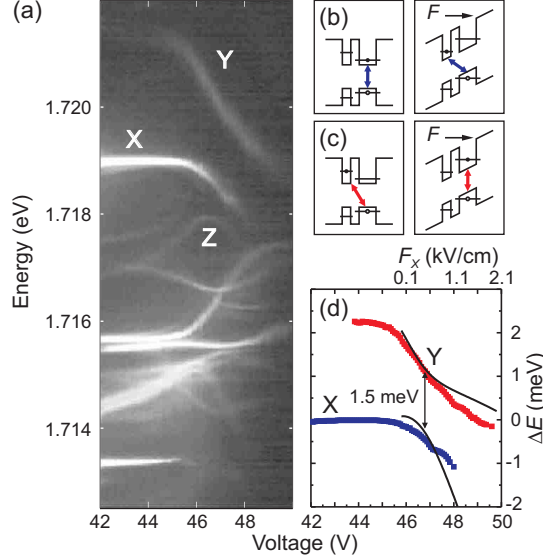


FIG. 4: (a) Intensity map obtained from PL spectra as a function of applied voltage for QDM A. (b)-(c) Schematic band diagrams with the relevant transitions at different electric field amplitudes for X and Y lines, respectively. (d) Peak positions of the X and Y lines observed in (a). Continuous lines represent the result of the calculation discussed in the text.

and also for single GaAs/AlGaAs QDs, has not been reported for other self-assembled QDs and is at present not understood. Most importantly, for larger fields, the PL spectra of some of the studied QDMs show pronounced red and blue-shifts leading to intricate patterns consisting of crossings and avoided crossings with increasing field. This is illustrated for QDM A in Fig. 4(a), which displays a PL intensity map obtained from a series of spectra collected at 6 K as a function of applied voltage (defined as $2 \times V_a$).

Since at present we are not able to identify unambiguously the origin of the other spectral lines, we concentrate on the behavior of the high energy side of the spectrum and in particular on the X and Y lines. At low bias, X corresponds to the direct neutral exciton X^0 transition. After the initial blue-shift, the onset of a strong red-shift is observed at an applied voltage of about 44.5 V. The intensity of the X line then drops below the detection limit. At low fields the spectral line Y is weak and can be assigned to an indirect exciton recombination. When the voltage is increased it gains in intensity and also red-shifts, but at a much larger rate compared to X. Figure 4(d) shows the X and Y peak position obtained by fitting the lines with Lorentzian functions. At the beginning (for applied voltages below 46.8 V), the splitting between these lines decreases. At a voltage of ~ 46.8 V, the two lines reach

a minimum energy splitting of 1.5 meV and then gradually separate. This anticrossing behavior, previously reported only for vertically-stacked QDs [4, 5, 6], demonstrates that the two GaAs QDs composing our lateral QDMs are quantum coupled. We can therefore interpret the energy splitting of 1.5 meV as the coupling energy. We also note that the pattern deviates slightly from a perfect anticrossing. In particular, the X line displays an anomalous shift at a voltage of about 48 V. This anomaly is probably due to interaction of the energy levels responsible for the X-Y transitions with other energetically close states [see, in Fig. 4(a), the line Z, which approaches X and avoids crossing it].

To obtain further insight into the anticrossing behavior, we perform a quantized energy calculation of the electron and heavy hole wavefunctions in a QD using a single band effective mass approximation. In this calculation, a truncated pyramidal shape is assumed for each GaAs QD in a QDM. First, the QD diameter is tuned to fit with the s -shell and p -shell separation. Then, the height of each QD in the QDM is adjusted to the ground state of the direct and indirect transition of the QDM A. The fitting of the anticrossing energy is obtained by tuning the lateral distance between the apex of each QD and varying the applied electric field strength F_X . A splitting energy of 1.5 meV is obtained when the separation distance is 31 nm, consistent with the value observed by AFM (35 ± 4 nm). Because of the large separation between the two QDs, we expect the indirect exciton to have a large polarizability and therefore display a pronounced QCSE at low fields. In the calculation the anticrossing is in fact observed at a field amplitude of only 0.45 kV/cm. The calculation also suggests that the coupling is mediated by electron tunneling since hole tunneling would yield smaller splitting energies. Schematic band diagrams of the involved transitions at different field amplitudes for lines X and Y are shown in Fig 4(b) and (c), respectively. By assuming a linear relation between the electric field and the voltage [$F_X = k \times (V_a - 22.9 \text{ V})$, $k=1000 \text{ cm}^{-1}$], we plot the calculated energies as continuous lines in Fig. 4(d). Since the model does not include all the states involved in the transitions observed experimentally, it can not reproduce the anomalous shifts. Moreover, the discrepancy between fit and experiment at high fields is due to the nonlinear relation between the field and the applied voltage [see Fig. 3(d)], a technical issue which may be solved by improving the contact structure as proposed in Ref. [26].

In conclusion, we have reported the fabrication of lateral GaAs QDMs and we have provided evidence of lateral coupling between the two nearby QDs. The quantum coupling is

controllably tuned by applying an in-plane electric field and manifests itself as an anticrossing pattern in the PL spectra. The coupling is likely to be mediated by electron tunneling, through which the states of direct and indirect exciton are brought into resonance by the electric field. While the present demonstration is based on a fully self-assembled structure, we envision the possibility of using lithographically positioned nanoholes [10, 27] as a template for the fabrication of QDMs with well-defined position. The application of an extra gate electrode above the barrier separating the two QDs may allow the coupling strength to be tuned [11].

The authors thank M. Riek and T. Reindl for help in the sample processing and K. v. Klitzing for continuous support and interest. The work was financially supported by the SFB/TR21, the BMBF (03N8711) and by the DFG research group “Positioning of single nanostructures - Single quantum devices”.

* Electronic address: l.wang@fkf.mpg.de

- [1] D. Loss and D. P. DiVincenzo, *Phys. Rev. A* **57**, 120 (1998).
- [2] G. Burkard, D. Loss, and D. P. DiVincenzo, *Phys. Rev. B* **59**, 2070 (1999).
- [3] F. H. L. Koppens, C. Buizert, K. J. Tielrooij, I. T. Vink, K. C. Nowack, T. Meunier, L. P. Kouwenhoven, and L. M. K. Vandersypen, *Nature* **442**, 766 (2006).
- [4] H. J. Krenner, M. Sabathil, E. C. Clark, A. Kress, D. Schuh, M. Bichler, G. Abstreiter, and J. J. Finley, *Phys. Rev. Lett.* **94**, 057402 (2005).
- [5] G. Ortner, M. Bayer, Y. Lyanda-Geller, T. L. Reinecke, A. Kress, J. P. Reithmaier, and A. Forchel, *Phys. Rev. Lett.* **94**, 157401 (2005).
- [6] E. A. Stinaff, M. Scheibner, A. S. Bracker, I. V. Ponomarev, V. L. Korenev, M. E. Ware, M. F. Doty, T. L. Reinecke, and D. Gammon, *Science* **311**, 636 (2006).
- [7] H. J. Krenner, E. C. Clark, T. Nakaoka, M. Bichler, C. Scheurer, G. Abstreiter, and J. J. Finley, *Phys. Rev. Lett.* **97**, 076403 (2006).
- [8] G. Bester and A. Zunger, *Phys. Rev. B* **72**, 165334 (2005).
- [9] A. S. Bracker, M. Scheibner, M. F. Doty, E. A. Stinaff, I. V. Ponomarev, J. C. Kim, L. J. Whitman, T. L. Reinecke, and D. Gammon, *Appl. Phys. Lett.* **89**, 233110 (2006).
- [10] O. G. Schmidt, C. Deneke, S. Kiravittaya, R. Songmuang, H. Heidemeyer, Y. Nakamura,

- R. Zapf-Gottwick, C. Müller, and N. Y. Jin-Phillipp, *IEEE J. Sel. Top. Quantum Electron.* **8**, 1025 (2002).
- [11] R. Songmuang, S. Kiravittaya, and O. G. Schmidt, *Appl. Phys. Lett.* **82**, 2892 (2003).
- [12] T. V. Lippen, R. Nötzel, G. J. Hamhuis, and J. H. Wolter, *Appl. Phys. Lett.* **85**, 118 (2004).
- [13] S. Suraprapapich, S. Thainoi, S. Kanjanachuchai, and S. Panyakeow, *J. Vac. Sci. Technol. B* **23**, 1217 (2005).
- [14] M. Hanke, M. Schmidbauer, D. Grigoriev, P. Schäfer, R. Köhler, T. H. Metzger, Z. M. Wang, Y. I. Mazur, and G. J. Salamo, *Appl. Phys. Lett.* **89**, 053116 (2006).
- [15] M. Yamagiwa, T. Mano, T. Kuroda, T. Tateno, K. Sakoda, G. Kido, N. Koguchi, and F. Minami, *Appl. Phys. Lett.* **89**, 113115 (2006).
- [16] J. H. Lee, Z. M. Wang, N. W. Strom, Y. I. Mazur, and G. J. Salamo, *Appl. Phys. Lett.* **89**, 202101 (2006).
- [17] G. J. Beirne, C. Hermannstädter, L. Wang, A. Rastelli, O. G. Schmidt, and P. Michler, *Phys. Rev. Lett.* **96**, 137401 (2006).
- [18] T. Unold, K. Mueller, C. Lienau, T. Elsaesser, and A. D. Wieck, *Phys. Rev. Lett.* **94**, 137404 (2005).
- [19] A. Rastelli, S. Stuffer, A. Schliwa, R. Songmuang, C. Manzano, G. Costantini, K. Kern, A. Zrenner, D. Bimberg, and O. G. Schmidt, *Phys. Rev. Lett.* **92**, 166104 (2004).
- [20] S. Kiravittaya, R. Songmuang, N. Y. Jin-Phillipp, S. Panyakeow, and O. G. Schmidt, *J. Cryst. Growth* **251**, 258 (2003).
- [21] M. Bayer, G. Ortner, O. Stern, A. Kuther, A. A. Gorbunov, A. Forchel, P. Hawrylak, S. Fafard, K. Hinzer, T. L. Reinecke, et al., *Phys. Rev. B* **65**, 195315 (2002).
- [22] D. Gammon, E. S. Snow, B. V. Shanabrook, D. S. Katzer, and D. Park, *Phys. Rev. Lett.* **76**, 3005 (1996).
- [23] W. Heller, U. Bockelmann, and G. Abstreiter, *Phys. Rev. B* **57**, 6270 (1998).
- [24] B. D. Gerardot, S. Seidl, P. A. Dalgarno, R. J. Warburton, D. Granados, J. M. Garcia, K. Kowalik, O. Krebs, K. Karrai, A. Badolato, et al., *Appl. Phys. Lett.* **90**, 041101 (2007).
- [25] The finite element method with a commercial software package (COMSOL Multiphysics) is used for this calculation.
- [26] V. Stavarache, D. Reuter, A. D. Wieck, M. Schwab, D. R. Yakovlev, R. Oulton, and M. Bayer, *Appl. Phys. Lett.* **89**, 123105 (2006).

- [27] S. Kiravittaya, M. Benyoucef, R. Zapf-Gottwick, A. Rastelli, and O. G. Schmidt, *Appl. Phys. Lett.* **89**, 233102 (2006).